

Spin Flips versus Spin Transport in Nonthermal Electrons Excited by Ultrashort Optical Pulses in Transition Metals

V. Shokeen, M. Sanchez Piaia, and J.-Y. Bigot*

Université de Strasbourg, CNRS, Institut de Physique et Chimie des Matériaux de Strasbourg, UMR 7504, 67034 Strasbourg, France

T. Müller, P. Elliott, J. K. Dewhurst, S. Sharma,[†] and E. K. U. Gross

Max-Planck Institut für Mikrostrukturphysik, Weinberg 2, D-06120 Halle, Germany

(Received 8 March 2017; published 8 September 2017)

A joint theoretical and experimental investigation is performed to understand the underlying physics of laser-induced demagnetization in Ni and Co films with varying thicknesses excited by 10 fs optical pulses. Experimentally, the dynamics of spins is studied by determining the time-dependent amplitude of the Voigt vector, retrieved from a full set of magnetic and nonmagnetic quantities performed on both sides of films, with absolute time reference. Theoretically, *ab initio* calculations are performed using time-dependent density functional theory. Overall, we demonstrate that spin-orbit induced spin flips are the most significant contributors with superdiffusive spin transport, which assumes only that the transport of majority spins without spin flips induced by scattering does not apply in Ni. In Co it plays a significant role during the first ~ 20 fs only. Our study highlights the material dependent nature of the demagnetization during the process of thermalization of nonequilibrium spins.

DOI: 10.1103/PhysRevLett.119.107203

In the late 1990s it was shown that femtosecond optical pulses interacting with magnetic matter leads to an ultrafast (time scale of ~ 100 fs) macroscopic reduction in the magnetization [1–3]. Several experiments have confirmed this finding and such a demagnetization has been broadly divided into two categories—thermal demagnetization caused by hot electrons [1–7] and all-optical demagnetization and switching [8] involving either noncompensated GdFeCo ferrimagnetic lattices [9], the inverse Faraday effect in garnets [10], or dichroic absorption in ferromagnetic multilayers [11]. As the controllability of spins with light might strongly impact technological applications, with consequences for magnetic storage, spintronics, all-optical switching, heat assisted magnetic recording, etc., this field of femtomagnetism has recently become highly active, using diverse experimental approaches such as terahertz spectroscopy [12,13], x-ray circular dichroism [14,15], or high harmonic generation [16].

Despite this flurry of activity, the underlying physics causing this ultrafast demagnetization still remains contested with some of the most prominent models used for explaining this demagnetization being the three temperature model [1,17], Elliott-Yafet scattering induced spins flips [18], nonthermal excitations [19], spin-orbit interaction induced spin flips [20–24], and superdiffusive spin transport [25,26]. This superdiffusive model relies on majority spin electrons diffusing away from (into the substrate) while minority spin electrons stay within the magnetic layers to cause a reduction in the moment. It is also very controversial as the results of the experiments by

Vodungbo *et al.* [27] have been interpreted to confirm the assumptions of the model while the experimental data of Schelleken *et al.* [28] contest the validity of the very same assumptions. In addition Eschenlohr *et al.* [29] have shown that hot electrons generated in a nonmagnetic Au layer influence the magnetization of an adjacent Ni film, concluding that spin transport rather than spin flips plays the major role in magnetic processes on the femtosecond time scale, thereby indirectly supporting the superdiffusive mechanism.

In this Letter we present a joint theory and experimental work in an attempt to resolve this controversy. Experimentally, systematic measurements of the ultrafast demagnetization and transport in Ni and Co thin films of different thicknesses using 10 fs optical pulses are performed. Magnetization dynamics is probed both at the front (where the laser pulse comes in) and at the back face of these magnetic films at various time delays. Theoretically, a full *ab initio* study of laser induced spin dynamics in Ni and Co films (of various thicknesses) using time dependent density functional theory [30] is performed. Both experiments and theory clearly suggest a highly material dependent nature of the underlying physics of light induced demagnetization. In Ni spin flips dominate the physics of demagnetization at all times, while in Co the situation is more complex with spin diffusion playing a significant role initially and spin flips dominating the physics beyond the first ~ 20 fs.

Experiment.—The experiments are performed with a modified pump-probe time resolved magneto optical setup (see Fig. 1 of the Supplemental Material [31]) using 10 fs

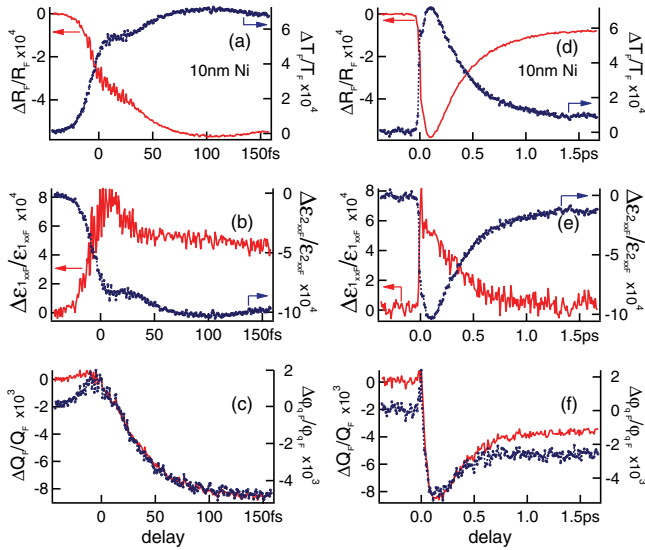


FIG. 1. Ultrafast magnetization dynamics of a 10 nm Ni film excited with 10 fs pump pulses. The sample is probed on the front face. Short delay dynamics of (a) reflectivity R_F (left axis) and transmission T_F (right axis). (b) Real and imaginary parts of the diagonal dielectric tensor $\epsilon_{1_{xxF}}$ (left axis) and $\epsilon_{2_{xxF}}$ (right axis). (c) Dynamics of the amplitude Q_F (right axis) and phase φ_F (left axis) of the complex Voigt “vector.” Panels (d)–(f) show the same quantities when the charges and the spins are relaxing to the lattice. The pump energy density is $5 \times 10^{-5} \text{ J cm}^{-2}$.

pump pulses focused onto the front face of the sample within a diameter of $40 \mu\text{m}$ and two 10 fs probe pulses focused on the front (F) and back (B) faces with a $30 \mu\text{m}$ diameter and a density of energy 10 times less than the pump. All beams are p polarized with an accuracy of $\pm 1^\circ$ with respect to the plane of incidence. The transmissions $T_{F,B}$, reflectivities $R_{F,B}$, Faraday rotations $\theta_{F,B}$, ellipticities $\eta_{F,B}$, and their corresponding time dependent differential quantities, with and without a pump beam, $(\Delta S_{F,B}/S_{F,B})(t)$ are measured as a function of the pump probe delay t . The temporal resolution is 0.5 fs using a grazing incidence mirror in the noncollinear pump-probe interferometer. Part of the reflected F and B probe beams are selected and interfere in a collinear Michelson interferometer to set the absolute arrival time of each pulse on the sample. The repetition rate of the laser is 80 MHz, centered at 810 nm with a maximum density of energy of 0.5 nJ/pulse for the pump. All static or dynamical measurements are performed for the two opposite directions ($\phi = 0^\circ, 180^\circ$) of a static magnetic field of 3.5 kOe perpendicular to the sample plane, $\phi = 90^\circ$. The direction of the initial unperturbed magnetization direction is obtained from the Stoner-Wohlfarth model. The Ni and Co thin films with thicknesses varying between 10 and 40 nm are grown by sputtering on a $500\text{-}\mu\text{m}$ -thick Al_2O_3 substrate and capped on the front face with 50 nm of Al_2O_3 .

The analysis of the experimental results requires us to proceed in several steps, briefly summarized hereafter and

described in more detail in the Supplemental Material [31]. The large spectral bandwidth of the pump and probe pulses requires us first to retrieve the complex refractive index or equivalently the diagonal complex tensor $\tilde{\epsilon}_{ii}$, $i = x, y, z$ from $R_{F,B}$ and $T_{F,B}$. The nondiagonal tensor elements $\tilde{\epsilon}_{ij}$, $i \neq j$, are obtained from the boundary and propagation matrices in magneto-optical multilayer films [32,33], including the substrate and capping layers. A similar procedure is used for extracting the dynamical differential quantities. For the magnetization, the ultimate interesting quantity is the complex Voigt vector defined as $\tilde{Q} = -i\tilde{\epsilon}_{ij}/\tilde{\epsilon}_{ii} = Qe^{i\varphi_q}$. The modulus Q is proportional to the magnetization. Let us emphasize that the validity of this assumption, extrapolating the Voigt model to the dynamical case, is consistent when the various parameters are assumed to be implicit functions of time in the linear response theory. To go further one has to consider the full time dependent third order polarization, including spins as performed, for example, in nonmetallic systems [22]. This is also the case for the coherent magneto-optical response, which requires considering the time ordering in the third order nonlinear response. Such refinements are beyond the scope of the present study. Naturally, all dynamical quantities are obtained from the differential measurements with and without a pump. $(\Delta Q/Q)(t)$ obtained from the polar signals is therefore directly comparable with the calculated projection $S_z(t)$ of the magnetization along the direction $0z$ perpendicular to the Ni or Co samples planes $0xy$ ($\phi = 90^\circ$).

As a typical representative set of measurements in a 10-nm-thick Ni sample, Figs. 1(a)–1(c) show at short time delays (up to 150 fs) the measured dynamical quantities $(\Delta R_F/R_F)(t)$, $(\Delta T_F/T_F)(t)$, $(\Delta \epsilon_{1_{xxF}}/\epsilon_{1_{xxF}})(t)$, $(\Delta \epsilon_{2_{xxF}}/\epsilon_{2_{xxF}})(t)$. $\epsilon_{1_{xx}}(t)$ and $\epsilon_{2_{xx}}(t)$ refer to the real and imaginary parts of the diagonal dielectric function. Similarly, we extract the nondiagonal parts $\epsilon_{1_{xy}}(t)$ and $\epsilon_{2_{xy}}(t)$ allowing us to obtain the time dependent magnetization $(\Delta Q_F/Q_F)(t)$, $(\Delta \varphi_{qF}/\varphi_{qF})(t)$. For this time scale up to 150 fs all differential quantities correspond to the thermalization dynamics of charges and spins. All curves are obtained for opposite magnetic fields and subtracted (added), and divided by 2, when they correspond to a quantity related to the nondiagonal (diagonal) tensor. Near the delay $t = 0$ the coherent spin-photon interaction is present [21], clearly visible here because of the 10 fs ultrashort pump and probe pulses. Then, the magnetization $(\Delta Q_F/Q_F)(t)$ decreases to its minimum [Fig. 1(c)]. Figures 1(d)–1(f) show the same quantities up to 1.6 ps when the charges and spins relax to the lattice, leading to a partial remagnetization [Fig. 1(f), left axis]. These three curves are typical of the usual “thermal remagnetization” that can be described by a three temperature model or with spin-phonon scattering. In contrast, the primary demagnetization induced by the 10 fs pulses clearly indicates that the

spin-phonon interaction may be discarded as already pointed out by Carva *et al.* [19].

Let us now compare the effects of spin flips versus superdiffusive spin transport in Ni and Co samples. Towards that goal we have probed four samples, Ni and Co each with thicknesses 10 and 40 nm, both on the front and back sides (the pump pulse exciting always the front side). We focus only on the modulus of Q ($\Delta Q_F/Q_F$)(t) (left ordinate axis) and ($\Delta Q_B/Q_B$)(t) (right ordinate axis) as they represent the magnetization dynamics. Figures 2(a) and 2(b) show the results for the 10 and 40 nm Ni films at short delays. Figure 2(c) shows the difference $\overline{\Delta Q/Q}(t)$ between the B and F faces. For the 10 nm film the demagnetization is larger on the back face (~ 1.9 times), indicating that superdiffusive spins have propagated forward, but this propagation is in both spin channels and not just the majority spins as stipulated by the superdiffusive model. In contrast, for the 40 nm film [Fig. 2(b)], the demagnetization is less on the back side (~ 0.7 times). This is better seen in Fig. 2(c), which clearly shows that for the 10 nm film the difference is negative while it is positive for the 40 nm film. Let us emphasize that all $\overline{\Delta Q/Q}(t)$ are negative quantities in this case [see Figs. 2(a) and 2(b)].

In the case of cobalt the situation is very different. Figures 2(d) and 2(e) show the results for the 10 and 40 nm Co films up to 300 fs. A clear sign inversion occurs during the first 50 fs on the B face of the 10 nm film. This proves that a significant proportion of majority spins have propagated without spin flips. Instead, for the thicker 40 nm Co

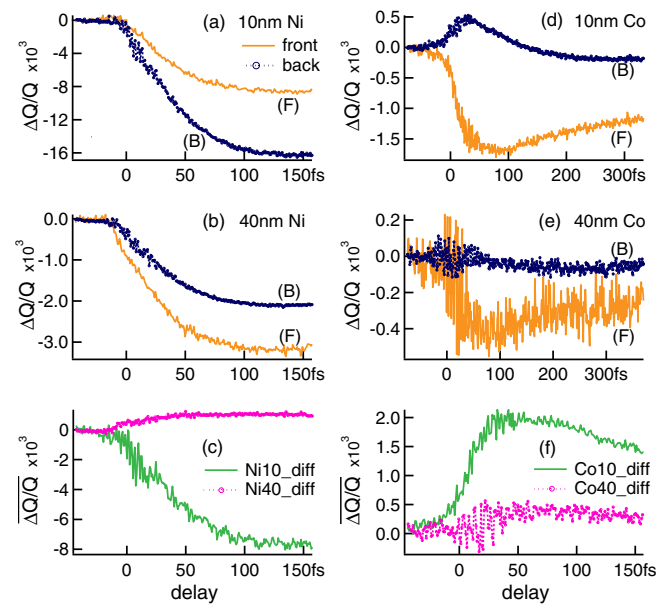


FIG. 2. Ultrafast magnetization dynamics of Ni and Co films excited with 10 fs pulses probed on their front (F) and back (B) faces. Nonthermal regime in (a) 10 nm Ni, (b) 40 nm Ni, (d) 10 nm Co, (e) 40 nm Co samples. Panels (c) and (f) are the differences between B and F faces for Ni and Co samples, respectively.

sample [Fig. 2(e)], the spin flips occur on both F and B faces, showing that the majority spins are flipped after some propagation distance which we estimate to be 25 ± 3 nm by performing the same measurements on a 25-nm-thick sample (not shown here). This is also apparent in the differences of the B and F faces displayed in Fig. 2(f) (again recall that the quantity plotted is $\overline{\Delta Q/Q}(t)$ for B and F). Thus, on the 10 nm Co film [Fig. 2(c)] one can see the contribution of the superdiffusive majority spins, which leads to the observation of a change in the sign of the magnetization in the early times.

Theory.—The superdiffusive model entails that the electrons in the majority spin channel are mobile and diffuse away from the magnetic layers while the electrons in the minority spin channel essentially remain in the magnetic layers, leading to a local loss in the magnetic moment. This is equivalent to saying that the average majority charge in the magnetic layers shows a strong decrease (due to the flow of majority spin current) as a function of time while the averaged minority charge stays pretty much constant. Despite totally neglecting the spin-orbit coupling, this model [25] successfully explained experimentally observed demagnetization in Ni. However, such a demagnetization can be reproduced using several other models as well [34,35], all of which rely on different underlying physics.

Given this, what one requires is a fully *ab initio* approach [36] that does not make any assumptions about the underlying physics or the system under investigation. In the present work we have performed such first principles calculations using time dependent density functional theory—spin-orbit coupling is included, spins are treated in a fully noncollinear way, and both of the spin channels are treated on the same footing [37]. This allows for the inclusion of spin current, spin diffusion, spin flips due to spin-orbit coupling, a restricted set of magnon excitations (by forming a supercell), and spin canting (for details see the Supplemental Material [31] and Refs. [23,38]). In Fig. 3 are presented the results for the layer averaged (over seven layers) change in the majority and minority charge as a function of time, $\Delta n(t) = n_{\text{maj/min}}(t) - n_{\text{maj/min}}(t=0)$ when all these processes are taken into account. From these results it is clear that the occupation of both the majority and minority spin electrons states changes significantly and contributes to the demagnetization process in magnetic films. This is in accordance with the experimental data of the present work and is in total contrast to the superdiffusive model.

In order to analyze these results, in Fig. 4 we present the total [Figs. 4(a) and 4(c)] and layer resolved [Figs. 4(b) and 4(d)] normalized moment for Ni and Co, $\{[M(t)]/[M(t=0)]\}$, as a function of time. The layer resolved results are obtained using two approaches: (1) by time propagating the full Hamiltonian in Eq. (1) of the Supplemental Material [31] and (2) by switching off the

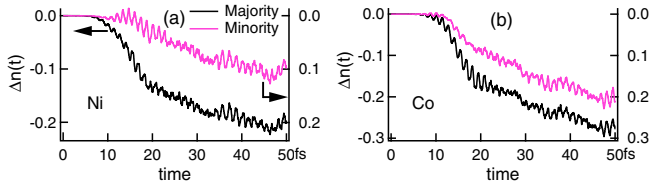


FIG. 3. Layer averaged majority (left axis) and minority (right axis) as a function of time (in femtoseconds). The results for Ni are shown in the left panel and for Co in the right panel. As compared to the $t = 0$ case there is a decrease in the majority and an increase in the minority spins.

spin-orbit coupling term [setting the last term to zero in Eq. (1) of the Supplemental Material [31]]. The later implies that demagnetization occurs only due to the flow of spin current from one part of the sample to another. This is similar to the scenario proposed by the superdiffusive model. In the former case, together with the spin current, spin flips and spin canting are also allowed. A comparison of the results from these two schemes would highlight the contribution of spin diffusion alone to the total demagnetization.

From the top panels of Fig. 4 it is clear that, like the experiments, we find Ni demagnetizes more than Co. The main reason for this is the fact that in Ni the d orbital is almost full and any change in the minority spin occupation leads to a large change in the moment. A similar effect leads to a large change in the moment on the Ni site also in the case of NiMnSb [24]. The lower panels of Fig. 4 show that in the case of Ni the demagnetization caused by the diffusion of spins alone strongly differs from the total

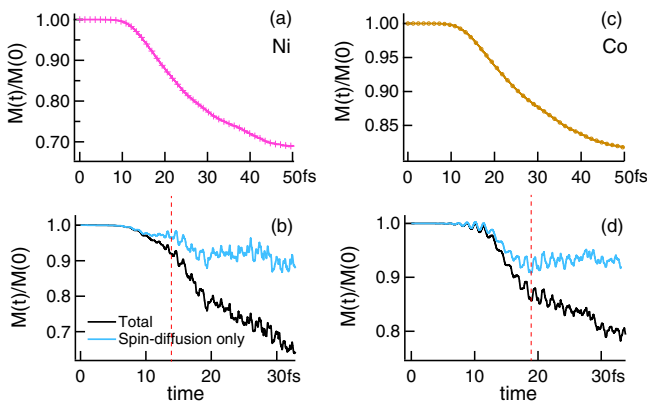


FIG. 4. Total (a),(c) and layer resolved (b),(d) normalized magnetic moment for Ni and Co films as a function of time (in femtoseconds). The layer resolved results are calculated in two ways: (1) by time propagating the full Hamiltonian in Eq. (1) of the Supplemental Material [31] (shown in black), and (2) by setting the last term to zero in Eq. (1) of the Supplemental Material [31] (shown in blue). The layer resolved data are for a representative layer (third layer) of a seven monolayer thick film. The vertical dotted lines in panels (b) and (d) show the time at which demagnetization due to spin diffusion starts to saturate.

demagnetization (which also includes the mechanism of spin flips). This indicates that, in the case of Ni, spin flips are the dominant mechanism for demagnetization. In the case of Co demagnetization with and without the spin-orbit coupling is similar during the initial elapse time of ~ 20 fs [see Fig. 4 (d)]. However, at times greater than 20 fs spin flips start to dominate the physics of demagnetization while spin diffusion begins to saturates. In this early time (< 20 fs), the magnetization dynamics in Co is thus different from Ni in that the diffusion of majority (as opposed to minority) spins contributes significantly.

This large temporal separation between the start of spin currents and spin flips in Co could explain the experimental findings of this work—in the early times a flow of spin current causes an accumulation of majority spins at the back face of Co films (leading to an increase in the moment) followed by spin flips becoming significant leading to a global demagnetization. In total contrast to this for Ni the temporal separation between spin currents and flips is small and spin flips, which cause a global demagnetization, dominate the physics of demagnetization. These results for Ni can explain not just the present experimental data but also the previous experimental work [28].

Conclusions.—In conclusion, we have performed joint theory and experimental work to study thin films of Ni and Co excited and probed with 10 fs pulses. Experimentally, a time resolved magneto-optical study is performed and the magnetization dynamics is studied from the amplitude of the Voigt vector. Using samples of different thicknesses we study the significance of spin flip versus the superdiffusive spin transport in the physics of demagnetization. Theoretically, we employ a state-of-the-art *ab initio* method (i.e., time-dependent density functional theory) to study the magnetization dynamics of Ni and Co films. From our work we conclude that (a) as opposed to superdiffusive spin transport, it is the spin flips that play the most significant role in the process of demagnetization in both Ni and Co, (b) experimentally the front faces of both materials display a demagnetization behavior as a function of time, (c) a sign inversion in the magnetization occurs at the back face of Co for early times ($t < 50$ fs), while the back face of Ni shows the same demagnetization behavior as its front face, and (d) this difference in the behavior between the back faces of Co and Ni in early times can be explained based on our theoretical results, which show a temporal separation between a significant amount of spin flips and majority spin diffusion in Co. In Ni, on the other hand, both of these processes occur at the same time. These results show that the demagnetization induced by femtosecond optical pulses in the two transition metals Ni and Co behave differently during the thermalization process of the spins.

J.-Y. B. and V. S. acknowledge the financial support of the European Research Council under the FP7-IDEAS-ERC program, project Advanced Grant ATOMAG: (ERC-2009-AdG-20090325 247452), and the Agence Nationale

de la Recherche in France, Equipex UNION (ANR-10-EQPX-52). S. S. and P. E. thank Deutsche Forschungsgemeinschaft through the SFB762 project and S. S. and T. M. thank the Deutsche Forschungsgemeinschaft, Schwerpunktprogramm 1840 (SPP 1840 QUTIF project).

*bigot@unistra.fr

†sharma@mpi-halle.mp.de

- [1] E. Beaurepaire, J.-C. Merle, A. Daunois, and J.-Y. Bigot, *Phys. Rev. Lett.* **76**, 4250 (1996).
- [2] J. Hohlfeld, E. Matthias, R. Knorren, and K. H. Bennemann, *Phys. Rev. Lett.* **78**, 4861 (1997).
- [3] M. Aeschlimann, M. Bauer, S. Pawlik, W. Weber, R. Burgermeister, D. Oberli, and H. C. Siegmann, *Phys. Rev. Lett.* **79**, 5158 (1997).
- [4] H.-S. Rhie, H. A. Dürr, and W. Eberhardt, *Phys. Rev. Lett.* **90**, 247201 (2003).
- [5] B. Koopmans, J. J. M. Ruigrok, F. D. Longa, and W. J. M. de Jonge, *Phys. Rev. Lett.* **95**, 267207 (2005).
- [6] A. B. Schmidt, M. Pickel, M. Wiemhöfer, M. Donath, and M. Weinelt, *Phys. Rev. Lett.* **95**, 107402 (2005).
- [7] I. Radu, G. Woltersdorf, M. Kiessling, A. Melnikov, U. Bovensiepen, J.-U. Thiele, and C. H. Back, *Phys. Rev. Lett.* **102**, 117201 (2009).
- [8] A. Kirilyuk, A. V. Kimel, and T. Rasing, *Rep. Prog. Phys.* **76**, 026501 (2013).
- [9] F. Hansteen, A. V. Kimel, A. Kirilyuk, and T. Rasing, *Phys. Rev. Lett.* **95**, 047402 (2005).
- [10] A. Kimel, A. Kirilyuk, P. A. Usachev, R. V. Pisarev, A. M. Balbashov, and T. Rasing, *Nature (London)* **435**, 655 (2005).
- [11] C.-H. Lambert *et al.*, *Science* **345**, 1337 (2014).
- [12] T. Kampfrath, A. Sell, G. Klatt, A. Pashkin, S. Mährlein, T. Dekorsy, M. Wolf, M. Fiebig, A. Leitenstorfer, and R. Huber, *Nat. Photonics* **5**, 31 (2011).
- [13] J. Walowski and M. Münzenberg, *J. Appl. Phys.* **120**, 140901 (2016).
- [14] C. Stamm *et al.*, *Nat. Mater.* **6**, 740 (2007).
- [15] C. Boeglin, E. Beaurepaire, V. Halté, V. López-Flores, C. Stamm, N. Pontius, H. A. Dürr, and J.-Y. Bigot, *Nature (London)* **465**, 458 (2010).
- [16] C. La-O-Vorakiat *et al.*, *Phys. Rev. Lett.* **103**, 257402 (2009).
- [17] J.-Y. Bigot, *C. R. Acad. Sci. Paris Ser. IV* **2**, 1483 (2001).
- [18] B. Koopmans, G. Malinovski, F. D. Longa, D. Steiauf, M. Fähnle, T. Roth, M. Cinchetti, and M. Aeschlimann, *Nat. Mater.* **9**, 259 (2010).
- [19] K. Carva, M. Battiato, D. Legut, and P. M. Oppeneer, *Phys. Rev. B* **87**, 184425 (2013).
- [20] G. P. Zhang and W. Hübner, *Phys. Rev. Lett.* **85**, 3025 (2000).
- [21] J.-Y. Bigot, M. Vomir, and E. Beaurepaire, *Nat. Phys.* **5**, 515 (2009).
- [22] H. Vonesch and J.-Y. Bigot, *Phys. Rev. B* **85**, 180407(R) (2012).
- [23] K. Krieger, J. K. Dewhurst, P. Elliott, S. Sharma, and E. K. U. Gross, *J. Chem. Theory Comput.* **11**, 4870 (2015).
- [24] P. Elliott, T. Mueller, J. K. Dewhurst, S. Sharma, and E. K. U. Gross, *Sci. Rep.* **6**, 38911 (2016).
- [25] M. Battiato, K. Carva, and P. M. Oppeneer, *Phys. Rev. Lett.* **105**, 027203 (2010).
- [26] M. Battiato, K. Carva, and P. M. Oppeneer, *Phys. Rev. B* **86**, 024404 (2012).
- [27] B. Vodungbo *et al.*, *Nat. Commun.* **3**, 999 (2012).
- [28] A. J. Schellekens, W. Verhoeven, T. N. Vader, and B. Koopmans, *Appl. Phys. Lett.* **102**, 252408 (2013).
- [29] A. Eschenlohr, M. Battiato, P. Maldonado, N. Pontius, T. Kachel, K. Holldack, R. Mitzner, A. Föhlisch, P. M. Oppeneer, and C. Stamm, *Nat. Mater.* **12**, 332 (2013).
- [30] E. Runge and E. K. U. Gross, *Phys. Rev. Lett.* **52**, 997 (1984).
- [31] See Supplemental Material at <http://link.aps.org/supplemental/10.1103/PhysRevLett.119.107203> for the experimental configuration of the time resolved magneto-optical setup, the methodology to retrieve the time dependent nondiagonal dielectric function as well as the Hamiltonian used in the time dependent density functional theory calculations.
- [32] J. Zak, E. R. Moog, C. Liu, and S. D. Bader, *J. Magn. Magn. Mater.* **89**, 107 (1990).
- [33] C. C. Robinson, *J. Opt. Soc. Am.* **54**, 1220 (1964).
- [34] P. M. Oppeneer and A. Liebsch, *J. Phys. Condens. Matter* **16**, 5519 (2004).
- [35] V. P. Zhukov, E. V. Chulkov, and P. M. Echenique, *Phys. Rev. B* **73**, 125105 (2006).
- [36] P. Hohenberg and W. Kohn, *Phys. Rev.* **136**, B864 (1964).
- [37] See J. K. Dewhurst, S. Sharma *et al.*, <http://elk.sourceforge.net> for information.
- [38] J. K. Dewhurst, K. Krieger, S. Sharma, and E. K. U. Gross, *Comput. Phys. Commun.* **209**, 92 (2016).